RECOVERING UTC (USNO,MC) WITH INCREASED ACCURACY USING A FIXED, L1-CA CODE, GPS RECEIVER

R. P. Giffard, Agilent Laboratories, Palo Alto, CA 94304, USA

Abstract

The accuracy with which a L1, single-frequency, GPS receiver can recover the time-scale UTC (USNO,MC) is well known to depend on many factors, including the accuracy of the signal in space, propagation path effects, the quality of the GPS/UTC (USNO,MC) correction, and the behavior of the receiver itself. Overall performance is now affected by a number of short- and medium-term noise sources that have hitherto been obscured by the intentional clock dither known as Selective Availability (SA). We report the development of a technique for periodically estimating the local ionospheric delay from observations of the code and carrier-phase GPS observables made with a multi-channel, L1, receiver module. An algorithm has been developed that uses information from several satellites to model the delay in real time. It is then possible to correct the raw time estimate from each satellite, improving the overall accuracy of the receiver's real-time estimate of GPS time or UTC(USNO,MC). With this technique it should be possible to approach the time accuracy obtained using a Precise Positioning Service (PPS) receiver. We have used a cesium standard ensemble related to UTC (USNO,MC) by common-view to measure the noise level obtained by applying the estimated corrections, and to compare this with the accuracy of the built-in single-frequency model.

1. INTRODUCTION

Single-frequency, L1, CA code, GPS receivers are often used to generate local time estimates synchronized either with the GPS system clock, or with UTC(USNO,MC). These receivers are modular, economical, and easy to operate. With a fixed receiver, and accurately known antenna coordinates, the time uncertainty can be minimized by averaging together individual time estimates from all of the satellites that are being tracked. This technique, which can be described as "Position-Hold, All-in-View," minimizes errors due to the accuracy of the "Signal in Space," multipath effects, and code correlator noise. Receivers operating in this way are often employed in "Disciplined Oscillators," which are widely used in telecommunications synchronization, calibration, science, and other applications [1,2].

Now that SA has been removed, the component of the inaccuracy in single-frequency time receivers that results from the effect of ionospheric delay has become more significant. Receivers can correct for the delay using a detailed model of the ionosphere, scaled by data contained in the 'navigation message' broadcast by the satellites. However, because of unpredictable variations of the ionosphere, this so-called single-frequency correction is only expected to absorb 50% of the effect. In timing receivers, the uncorrected ionospheric delay causes periodic daily time errors with amplitudes that change over a characteristic time of a few days. This unpredictable effect can cause significant errors in timing systems such as disciplined oscillators, and is of increasing importance with the approach of the solar activity maximum. In a previous publication [3] we have reported evidence for short-term and long-term errors at the level of 10 to 20 nanoseconds in disciplined oscillators that use the single-frequency model.

For users who are not qualified for the PPS, it is useful to explore ways of reducing the magnitude of ionosphere errors in single-frequency receivers. It is well known [4,5] that the

effect of many noise sources can be reduced by using the Common View (CV) technique, which is analogous to the use of differential GPS corrections (DGPS). The CV time transfer technique requires data exchange between the user and a reference station with a traceable time-scale. Since the technique does not easily work in real time, it requires the user to have a stable local clock. Uncorrected ionosphere effects are still important in common-view time transfer measurements over long baselines, although corrections can be applied after a delay of several days by using post-processed estimates from various sources, such as the IGS. The GLONASS system allows two-frequency operation, and is not encrypted. The GLONASS system is not synchronized with UTC or GPS time, and GLONASS time receivers are not yet economically available.

In this paper we will describe a technique for accurately estimating the local ionospheric delay using the GPS observables from an L1-C/A single-frequency receiver. The ionosphere estimate, which is made in near real time, is used to correct the averaged single-satellite time estimates and improve the accuracy of the receiver's time output. We will report measurements of the noise level obtained by comparison with a local time standard consisting of an active ensemble of two 5071A cesium standards referenced to UTC(USNO,MC) by common view. The measured real-time ionospheric delay was found to agree very well with the post-calculated "IONEX" products generated by the International GPS Service (IGS) network. The stability of the corrected time output indicates that the effect of the ionospheric delay has been reduced by at least an order of magnitude.

The technique that we have developed can be used to improve the performance of autonomous single-frequency time-transfer systems such as disciplined oscillators. The technique could also be used to improve the accuracy of common-view time transfer, particularly when the latency involved in using post-processed ionosphere results is objectionable. The technique requires some computation, but this can be performed in background because the ionosphere effect changes relatively slowly. A preliminary description of this work has been given elsewhere [6].

2. SINGLE-FREQUENCY IONOSPHERIC DELAY ESTIMATION

It is well known [7] that GPS code and phase ranges at a given frequency are affected with opposite signs by the dispersion due to free electric charges is the ionosphere. This principle has been used by Cohen et al. [8], and Tretheway et al. [9] to estimate the ionospheric delay using L1, single-frequency, observables. We have extended this work, and have developed a technique that is capable of generating an accurate estimate in real time. The new method uses the observables from several satellites to estimate the local ionospheric delay and its dependence on latitude and longitude with reduced uncertainty.

If the ionosphere is modeled as a thin slab, the expected difference Δ_i between the measured L1 code and carrier ranges for the i^{th} satellite, measured in meters can be written in the form:

$$\Delta_i = 0.325 \cdot F_i \cdot I + P_i + \varepsilon_i. \quad (1)$$

In this equation, I is the total electron content integrated along a vertical path through the ionosphere in 'TEC units' (10^{16} electrons per m^2). F_i is a dimensionless obliquity factor given by $1/\mathrm{Cos}(\theta)$, where θ is the angle between the normal to the ionosphere and the line of sight to the satellite. P_i is equal to an integer number of L1 wavelengths, and remains constant as long as phase-lock on the satellite signal is not lost. Receiver noise and multipath effects are represented

by the noise term ε_i. The code-carrier divergence Δ_i is easily calculated from the GPS observables output by a suitable receiver.

Although F can be calculated from the elevation angle of the satellite, Equation(1)cannot be used to calculate I directly because of the unknown constant P_i. Cohen et al [8] have shown that I can be determined by fitting the observed time dependence of the divergence to the variation of F in a solar-fixed, rotating frame, in which I can be considered effectively constant. Tretheway et al, [9] have reported the possibility of a real-time calculation of I using a Kalman filter technique.

In the technique that we have previously described [6], we used the time dependence of the observed divergence, removing the constant phase uncertainty. For a continuously tracked satellite:

$$d\Delta_i/dt = 0.325 \cdot (I \cdot dF_i/dt + F_i \cdot dI/dt) + d\varepsilon_i/dt. \quad (2)$$

At least four satellites can usually be tracked simultaneously, giving a set of simultaneous equations, each of the form of Equation (2). For each satellite, the rate of change of Δ_i can be estimated from the GPS observables, and the values of F_i and dF_i/dt can be calculated from the satellite ephemeris. As long as two or more satellites are tracked, estimates of I and dI/dt may be determined by the usual process of inverting the set of equations. It is interesting to note that, unlike dual-frequency methods, the calculation of I by this method is independent of satellite and receiver inter-frequency biases. The method does, however, depend on the assumption of a slab model for the ionosphere.

The algorithm described above assumes that the ionosphere is effectively uniform over the area covering the points at which it is "pierced" by the lines of sight from the receiver to the satellites. We have now extended the method to allow the value of I to depend in first order on latitude and longitude. The variation with longitude can be found by assuming that most of the variation of I with time is associated with the effect of earth rotation with an ionosphere distribution that is changing relatively slowly in the solar-fixed frame. The rate of change with time in earth-fixed coordinates is then approximately equal to the rate of change with longitude multiplied by the rate of rotation of the earth.

The line of sight from the satellite to the receiving antenna passes through the idealized height of the ionosphere slab at a "pierce" point that is generally offset in longitude and latitude from the position of the receiver. If the offsets for the i^{th} satellite are λ_i and ϕ_i respectively, and the local variation of I is characterized by derivatives $dI/d\lambda$ and $dI/d\phi$ respectively, the divergence is given by:

$$\Delta_i = 0.325 \cdot F_i \cdot (I + \lambda_i \cdot dI/d\lambda + \phi_i \cdot dI/d\phi) + P_i + \varepsilon_i. \quad (3)$$

In this equation, I is the vertical TEC value at the position of the receiver, and it is assumed that the geometry may be treated as rectangular. This assumption should be satisfactory for mid latitudes.

To find the equivalent of Equation (2), we differentiate Equation (3). Keeping only first-order derivatives, and putting $dI/dt = \Omega \cdot dI/d\lambda$, where Ω is the rate of rotation of the earth we obtain:

$$d\Delta_i/dt = 0.325 \cdot (I \cdot dF_i/dt + dI/d\lambda \cdot \{F_i \cdot [\Omega + d\lambda_i/dt] + \lambda_i \cdot dF_i/dt\} + dI/d\phi \cdot \{F_i \cdot d\phi_i/dt + \phi_i \cdot dF_i/dt\}) + d\varepsilon_i/dt. \quad (4)$$

There are now three unknowns: I, $dI/d\lambda$, and $dI/d\phi$. As before, with N satellites tracked, there are N such equations, which can be written in the form of a single matrix equation:

$$V = \mathbf{W} \cdot G. \quad (5)$$

In Equation (5), V is a column vector containing the measured values of $d\Delta_i/dt$ for the N satellites normalized by the factor 1/0.325, **W** is the N x 3 matrix containing the calculated geometrical coefficients for the N satellites, and G is a column vector whose elements are the unknowns:

$$G = (I, dI/d\lambda, dI/d\phi)^T. \quad (6)$$

If N is equal to or greater than three, the set of equations can be inverted to obtain I, $dI/d\lambda$ and $dI/d\phi$. The least-squares solution is described by the matrix equation:

$$G = [\mathbf{W}^T\mathbf{W}]^{-1}\mathbf{W}^T \cdot V. \quad (7)$$

The values of I, $dI/d\lambda$, and $dI/d\phi$ obtained from the solution are uncertain due to noise on the code-carrier differences. This is caused by receiver code correlator noise, and multipath noise that mostly affects the code ranges. The resulting noise on the output vector G can be estimated from the properties of the matrix $[\mathbf{W}^T\mathbf{W}]^{-1}\mathbf{W}^T$. Under the simplifying assumption that the noise on the output quantities is not correlated, the mean square output noise is proportional to the diagonal elements and the rms noise on the divergences. Experimental data show that the magnitudes of the elements are, generally, slowly changing functions of the satellite constellation geometry. From time to time, the geometry becomes less satisfactory for determining one or more of the output quantities. This condition is associated with the appearance of unusually large values of the diagonal elements.

3. TESTS OF THE ALGORITHM

The system used in the experiments to be described consists of an 8-channel, modular, C/A code receiver [10] fed by a choke-ring antenna. As discussed elsewhere [6], the receiver's crystal oscillator is phase-locked to an external frequency standard in order to make it easier to detect loss of phase lock. Raw data from the receiverareprocessed on-line by an external computer. The program calculates the code and phase ranges each second, and smoothes the code-carrier divergences using a filter with a pole frequency of 0.067 radian per second. Each 15 seconds, the value of the filtered divergence, the obliquity, the latitude offset, and the longitude offset for each satellite are stored in an array in memory. Pointers are maintained to indicate the start and finish of continuous tracking for each satellite.

Every 10 minutes, the stored data from all satellites that have been continuously tracked during the preceding 2400 seconds are analyzed in the on-line computer. Linear regressions of length

2400 seconds are used to estimate the rate-of-change of the code-carrier divergence and the rate-of-change of the obliquity. The obliquity and the offsets $d\lambda$ and $d\phi$ are averaged over the same interval. This data are then used to calculate the unknown vector G using the matrix relationship given in Equation (7). Although linear regressions may not be optimal for determining the rate of change, they are used in preference to IIR filters, because there is no settling time. The chosen length of the linear regressions represents a compromise between data latency and noise.

Comparing the noise variances on I and dI/dt (equal to $\Omega \cdot dI/d\lambda$) shows that a filter whose output approaches the integral of dI/dt in the short term, and the value of I in the long term can be used to reduce the noise on the estimate. A robust filter was devised to implement this principle using a cross-over time of 1 hour. The magnitudes of the diagonal elements of the matrix are used to determine whether the filter uses the current input quantities or values extrapolated from times at which the noise was satisfactory. The filter algorithm is based on the code-carrier smoothing filter typically used in GPS receivers.

To evaluate the performance of the filter and the algorithms described by Equations (1)-(7), stored raw GPS data were used to emulate the ionosphere delay given by the GPS built-in single-frequency model. In selected raw data files, the measured code-carrier differences for each satellite were replaced by calculated values obtained by doubling the delay given by the model [11] using the actual values of the satellite elevation and azimuth. The α and β parameters in the model were given the values contained in the satellite navigation message at the time. This modified raw data were then processed and filtered by the algorithms that were used for real-time data processing. The recovered variation of I was compared with values calculated directly using the model.

The success of the method is indicated by the data shown in Figure 1. The estimate of I found by the algorithm is in good agreement with the directly calculated value. It is clear that the use of a 2400-second processing span does not lead to serious rounding, although some ringing seems to occur where the second derivative of I is large. A linear regression between the two sets of data indicates that the values returned by the algorithm are smaller by a factor of 0.955. This may result from the use of a first-order time model. When there is no curvature, the model values are reproduced exactly by the algorithm. This is felt to be a good test of the data processing algorithm because the model represents the typical time variation of I, and the coefficient matrix values correspond to real satellite constellations.

When unmodified receiver raw data were processed in real-time, estimates of the three parameters included in the output vector G were obtained at 10-minute intervals. The outputs of the robust filter were written to a file. Data obtained over a 15-day period were used for a comparison with the IONEX ionosphere maps generated by the IGS from a worldwide array of dual-frequency receivers. The IONEX data could usually be obtained by Internet ftp after about 7 days. The data were interpolated for the latitude and longitude of the receiver at time intervals corresponding to 32 points per day.

Figure 2 shows a comparison between the output of the real-time single-frequency algorithm discussed above and the IGS data from the CODE center for a 13-day period. An ionosphere slab height of 450 km is assumed in both calculations. For the data shown, the agreement is very good. For the entire 15-day period for which both measurements are available, the mean difference is -0.52 TEC units, and the rms difference is 3.8 TEC units. There was no significant difference between the estimates from the two single-frequency receivers used, showing that

receiver noise had a negligible effect. The noise on the solution is probably mainly due to multipath effects.

4. CORRECTING THE RECEIVER TIME OUTPUT

Each second, the GPS receiver averages satellite tracking data to estimate the bias between its internal clock and GPS time. At the next second, this result is communicated to the user when the receiver emits a timing pulse aligned as closely as possible with the exact second. If the receiver is set to output UTC time, it applies the UTC/GPS correction contained in the navigation message, thereby relating the time of the output pulse to UTC(USNO,MC). To compensate the output using the measured ionospheric delay, the system calculates the amount by which the receiver output pulse has been delayed using the values of I, $dI/d\lambda$, and $dI/d\phi$. The result is provided numerically to the user, who can then use it to correct the result of the measurement of the time difference between the receiver output pulse and the 1 PPS pulse of the time-scale to be synchronized. The correction δt is given by a summation over the N satellites that are in the time solution for that second:

$$\delta t = 0.5416 \cdot F_i \cdot \Sigma (I + dI/d\lambda \cdot \lambda_i + dI/d\phi \cdot \phi_i) / N. \quad (8)$$

In these experiments, the time differences are averaged over the 600-second intervals between calculations of the ionospheric delay parameters. It is necessary to calculate a correctly averaged correction using the ionosphere values propagated to the mid point of the averaging interval, which is done as follows. The geometrical quantities F_i, $F_i \cdot \lambda_i$, and $F_i \cdot \phi_i$ are calculated each second, averaged over the satellites that are currently in the time solution, and stored in memory. After 600 seconds, the average of the accumulated counter readings is calculated. The averages of the three geometrical quantities over the previous 600 seconds are used with the delay parameters to calculate the estimated correction to the averaged time-difference, δt^*:

$$\delta t^* = 0.5416 \cdot (I \cdot \Sigma \langle F_i \rangle + dI/d\lambda \cdot \Sigma \langle F_i \cdot \lambda i \rangle + dI/d\phi \cdot \Sigma \langle F_i \cdot \phi_i \rangle)/600. \quad (9)$$

In this equation, triangular brackets denote averaging over the satellites that are used by the receiver in the time solution for a given second, and the summation is carried out over the most recent 600 solutions. The ionosphere estimates, the number of satellites in the estimate, the raw counter average, the counter rms, and the counter average corrected by δt^* are included in the file output.

5. TIME STABILITY EXPERIMENTS

To evaluate the success of the method, the time-differences between a local time-scale and the 1PPS outputs of the two receiver systems using the real-time ionosphere correction were measured for several weeks. One receiver was set to output UTC(USNO,MC) via GPS and the other was set to output GPS time. The built-in ionosphere correction was turned off in both of these receivers. The raw time differences, the real-time ionosphere estimates, and the corrected time differences were logged at 10-minute intervals. The time difference was also recorded for a conventional receiver system using the GPS single-frequency ionosphere correction. An independent receiver was used to log page 18, sub-frame 4, of the navigation message so that the current GPS-UTC correction and the ionosphere model parameters could be obtained for comparison. All receivers used the same choke-ring antenna.

The local time-scale consisted of an active ensemble of two high performance 5071As that was disciplined to UTC(USNO,MC) by a feedback loop with a time constant of 10 days. The time-difference between the 1 PPS output of the local ensemble and UTC(USNO,MC) was determined by common-view measurements as described elsewhere [3]. About 35 common-view passes could be compared daily using the BIPM USA (east coast) schedule. In the time comparison experiments to be described, a correction for the local time-scale was obtained by smoothing the common-view differences using a sliding filter with triangular weighting and a peak-to-peak width of 2 days [3].

The upper curve in Figure 3 shows the variation of the time difference between the corrected local time-scale and the raw output of a receiver with the GPS single-frequency model disabled, and the GPS/UTC correction enabled. The data have been shifted up by 50 ns for clarity. The time difference is dominated by the daily variation of the ionospheric delay, which has a fairly constant peak-to-peak amplitude during this period. The amplitude of the component at one cycle-per-day was determined by Fourier analysis to be 26 ns with a phase corresponding to a daily maximum at 21:05 UT.

The lower curve in Figure 3 shows the measured time difference for the same period between the corrected local time-scale and the receiver with the GPS single-frequency model and the GPS/UTC correction enabled. Daily effects can be seen, suggesting that the built in ionosphere correction was not completely effective at this time. The effects are significantly bi-modal, corresponding to the rising and falling edges of the actual delay. It appears that the effect is due to a phase difference between the real ionosphere delay, shown in the upper curve, and the single-frequency correction, which has a maximum at 22:14 UT at the longitude of the receiver, −122.15 degrees. This effect is characteristic of the data during this particular period, and is not always observed.

Correcting the measured raw time difference according to Equation (9), using the ionosphere model calculated in real-time, was found to reduce the effect of the ionosphere delay by a factor of 10, or 20 dB. Fourier analysis showed that, after correction, the time difference still contained a 1 cycle-per-day (cpd) component in phase with the original ionosphere effect. For both of the receivers studied, the 1 cpd component was minimized if the average correction δt^* was increased by a factor of 1.10. The rejection was then about 26 dB.

There are several possible explanations for this unexpected result. The results, shown in Figure 1 indicate that the algorithm has an effective scale factor of 95.5% when typical emulated data are used. It might be expected that the correction would have to be increased by about the reciprocal of this factor. Further inaccuracy may result from the use of a simple slab model for the ionosphere. Recent work has attempted to extend the ionosphere model to include its distribution with respect to height [12]. There is currently great interest in the use of advanced ionospheric models for aircraft navigation, but it is not yet clear how they would affect the compensation of a time receiver. The agreement between the ionospheric parameters and the IGS model is not surprising because both calculations are base on a slab ionosphere model with a height of 450 km. It should be pointed out that the accuracy of the IGS orbital and geodetic results does not depend on the ionosphere model used because the ionosphere delay is removed directly by dual-frequency ranging.

An alternative explanation is that some other daily variation such as a daily environmental change in the system group delay was being compensated. This seems unlikely because of the

stability of the effect, and its accurate agreement in phase with the ionosphere maximum. The same argument can be used with respect to any possible multipath effect, which would also have a 1 cpd periodicity.

Figure 4 shows the time differences with respect to the corrected local time-scale for the two receiver systems using real-time ionosphere correction increased by the experimentally determined factor 1.10. The upper curve is for the receiver operating in GPS time, and the data have been shifted up by 40 ns for clarity. (The 13-second integer time-difference between GPS time and UTC does not affect the data, which are modulo 1-second.) The data show a slow run-out of about 20 ns peak-to-peak between the local time-scale corrected to UTC(USNO,MC) and the receiver output during 14 days. The lower curve shows the time difference between the corrected local time-scale and the output of the ionosphere corrected receiver using the UTC/GPS correction. The data show significantly less long-term run-out, but the short-term variation appears to be less smooth. This is possibly due to the step-wise evolution of the GPS/UTC correction. The overall rms deviation over the 14-day period is 5 ns. Fourier analysis shows that the remaining amplitude at 1 cpd is less than 1 ns. Possible remaining sources of noise include satellite ephemeris errors, including clocks, and multipath effects. The magnitude of the noise is consistent with recent measurements of the accuracy of the signal in space [14].

The absolute values of the time-differences shown in Figures 3 and 4 are not significant. The CV receiver system has been accurately calibrated at NIST, but no attempt has been made to calibrate the absolute delays of the other receivers.

6. SUMMARY

We have demonstrated that the local GPS L1 ionospheric delay can be accurately estimated in real time with a single-frequency receiver by using the GPS observables from several satellites. The TEC values obtained assuming a slab ionosphere model at 450 km compare well with data from the IONEX maps produced by the IGS network. Our method currently involves averaging the raw data over 2400 seconds to minimize noise, and this does not seem to reduce the accuracy of the estimate significantly.

We have shown that the real-time delay estimate can be used to reduce the short-term effect of the ionosphere on the output of a single frequency time receiver. To optimize the correction of the ionospheric delay, it was found necessary to increase the magnitude of the delay estimate by a factor of 1.10. The reason for this is not yet completely understood, but it may be due to the use of a simple slab ionosphere model, and the neglect of second order time differences. This effect could possibly be studied by analyzing code-carrier divergences flattened with the calculated ionosphere model. At the latitude of the experiment, 37.68 degrees, the amplitude of the daily ionosphere effect could be reduced by 26 dB. More experiments would be useful to find out whether long-term effects that we have reported elsewhere [3], are also reduced.

In these experiments, a time correction was calculated every 10 minutes and applied to the average of the time differences measured over the same period. In an application such as a disciplined oscillator, where a less stable local clock must be steered, it would be possible to correct the time difference much more frequently without significantly increasing the computational load.

7. ACKNOWLEDGMENTS

It is a pleasure to acknowledge the enthusiastic support of Len Cutler, and the encouragement of the Precision Instrumentation Group at Agilent Laboratories. Ray Wong constructed the phase-lock circuitry.

8. REFERENCES

[1] J.A. Davis and J. M. Furlong, "Report on the Study to Determine the Suitability of GPS Disciplined Oscillators as Time and Frequency Standards Traceable to the UK National Time-scale UTC (NPL)," Center for Time Metrology, National Physical Laboratory, Middlesex, TW11 0LW, U.K.

[2] R.P.Giffard and R. Pitcock, "An Accurate Local Traceable Time-Scale for Calibrating GPS Time-Transfer Products," Proceedings of the Workshop and Symposium of the NCSL, Toronto, Canada, July 2000.

[3] R.P. Giffard and R. Pitcock, "Comparison of Common-View and One-Way GPS Time Transfer Over a 4000 km East-West Baseline," Proceedings of the 31st Annual Precise Time and Time Interval (PTTI) Systems and Applications Meeting, Dana Point, California, USA, Dec. 1999, pp. 393-404.

[4] D.W. Allan, D.D. Davis, M. Weiss, A. Clements, B. Guinot, M. Granvaud, K. Doren-wendt, B. Fischer, P. Hetzel, S. Aoki, M-K. Fujimoto, L. Charron, and N. Ashby, "Accuracy of International Time and Frequency Comparisons Via Global Positioning Satellites in Common-View," IEEE Trans. Inst. and Meas., Vol IM-34, 1985, pp. 118-125.

[5] W. Lewandowski, "GPS Common-View Time Transfer," Proceedings of the 25th Annual Precision Time and Time Interval (PTTI) Applications and Planning Meeting, Marina Del Rey, USA, Dec. 1994, NASA Conference Publication 3267, pp. 235- 245.

[6] R.P. Giffard, "Estimation of Ionospheric Delay Using L1 Code and Carrier Phase Observables," Proceedings of the 31st Annual Precise Time and Time Interval (PTTI) Systems and Applications Meeting, Dana Point, California, Dec. 1999, pp. 405-417.

[7] J. A. Klobuchar, "Ionospheric effects on GPS", in Global Positioning System: Theory and Applications, Vol., Editors: B.W. Parkinson and J.J. Spilker, Progress in Astronautics and Aeronautics, Vol. 163, pp. 485-515.

[8] C.E. Cohen, B. Pervan, and B.W. Parkinson, "Estimation of Absolute Ionospheric Delay Exclusively through Single-Frequency GPS Measurements," Proceedings of ION GPS-92, Institute of Navigation 1992, pp. 325-330.

[9] M.L. Tretheway, I. Catchpole, and A. Hansla, "Single Frequency Ionosphere Determination Using GPS," Proceedings of ION GPS-93, Salt Lake City, UT, USA, Institute of Navigation 1993, pp. 1373-1381.

[10] Motorola ONCORE-VP, 8-channel receivers with firmware versions 8.9 and 10.0 were used in this work. This receiver is currently obsolete, but any receiver with suitable outputs can be used.

[11] GPS Interface Control Document ICD-GPS-200, Revision IRN-200C-002, Arinc Research Corporation, 10 Oct. 1993, pp. 124-127.

[12] A.J. Hansen, "Real-time Ionospheric Tomography Using Terrestrial GPS Sensors," Proceedings of ION GPS-98, Nashville, TN, USA, Institute of Navigation 1998, pp. 717-727.

[13] Robin P. Giffard, "Ionosphere Effects at the Nanosecond Level Observed in Common-View Time-Transfer," Navigation, Vol. 44, N0. 4, Winter 1997-1998, pp. 489-497.

[14] Donghai Dai, Todd Walter, Per Enge, and J. David Powell, "Satellite-Based Augmentation System Signal-In-Space Integrity Performance Analysis, Experience, and Perspectives," Proceedings of ION GPS-99, Kansas City, MO, USA, September 1999.

9. FIGURES

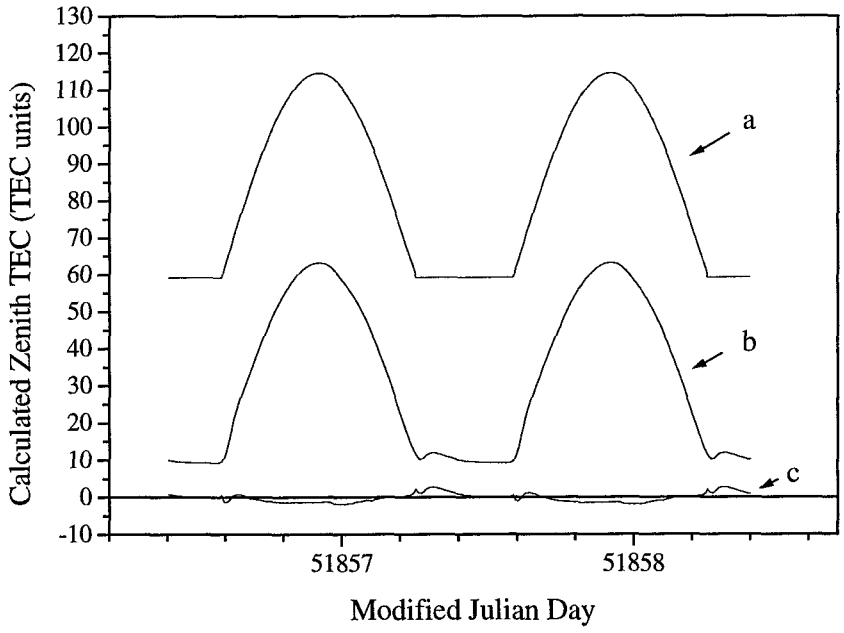

Figure 1. Curve a: Zenith TEC value calculated using the GPS single-frequency model. (Data shifted up 50 TEC units for clarity.) Curve b: The zenith TEC calculated by the real-time ionosphere algorithm from raw data emulating the single-frequency model, with the same values of α and β (from the current navigation message). Curve c: The difference between curves b and a.

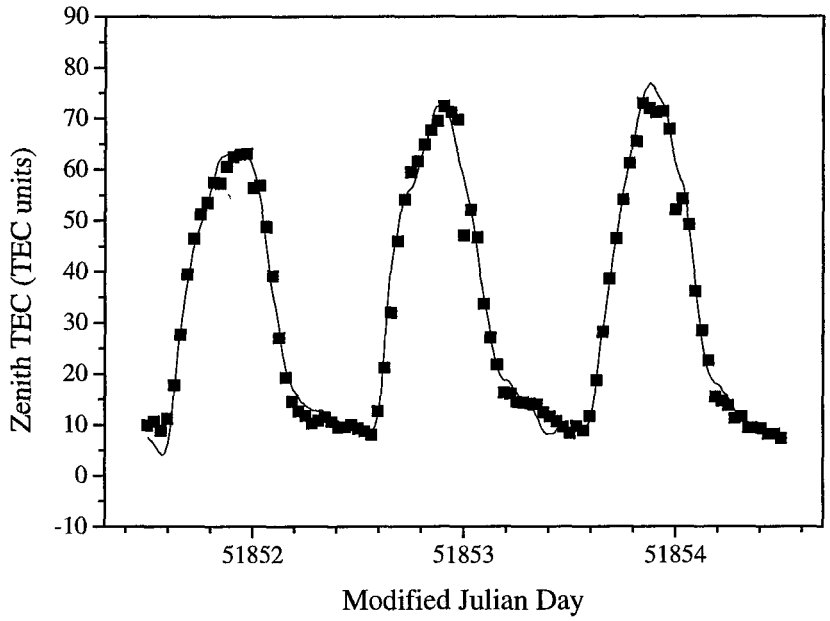

Figure 2. The figure shows a comparison between the output of the single-frequency algorithm and IGS data. The solid curve is the filtered output of the algorithm, calculated in real-time. The solid points represent IONEX data obtained about 7 days later from the IGS Berne computation center (CODE), interpolated to the latitude and longitude of the single-frequency receiver at a rate of 32 points per day.

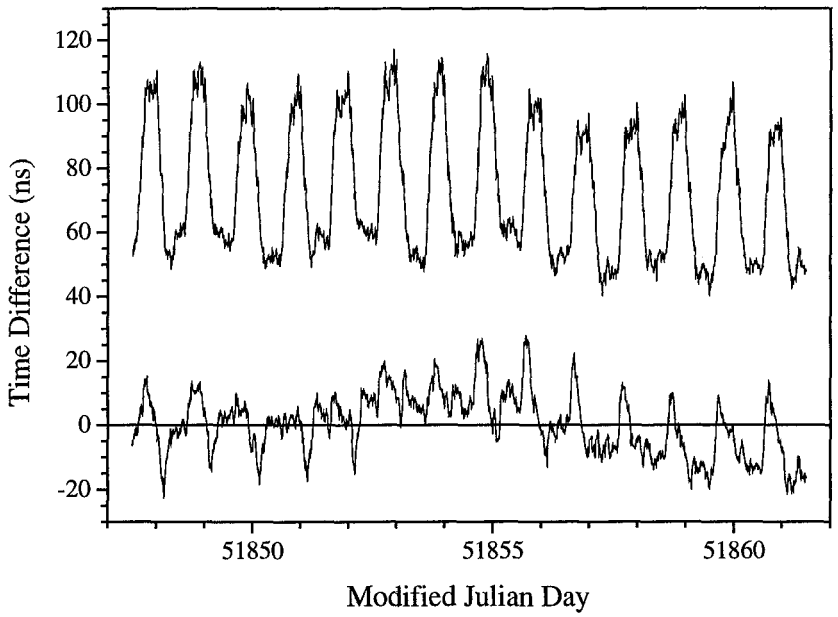

Figure 3. Upper curve: The measured time difference between the corrected local time-scale and the raw output of a receiver using no ionosphere compensation. The GPS/UTC correction is enabled. (Data shifted up by 50 ns for clarity.) The time difference is dominated by the daily variation of the uncorrected ionospheric delay. The lower curve shows the corresponding time-difference for a receiver with the GPS single-frequency model enabled.

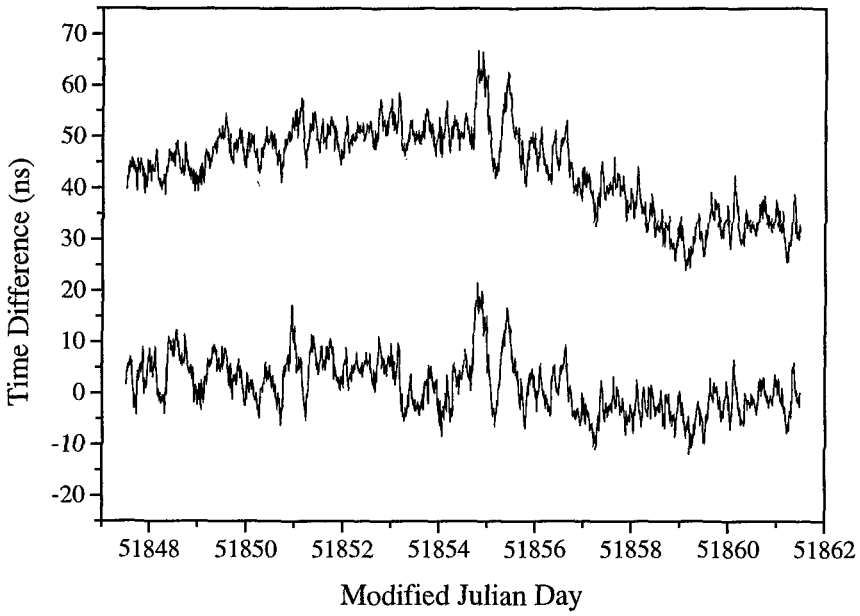

Figure 4. Time differences between the corrected local time-scale and the 1 PPS outputs of two receivers compensated using the real-time ionosphere estimation technique. The magnitude of the compensation has been enhanced by a factor of 1.10, as discussed in the text. Upper curve: UTC/GPS correction disabled. (Data shifted up 40 ns for clarity.) Lower curve: UTC/GPS correction enabled. The data are composed of 10-minute averages, and the absolute values of the time differences are not significant.

Questions and Answers

THOMAS CLARK (NASA Goddard Space Flight Center): What was the receiver and firmware?

ROBIN GIFFARD: Motorola Oncore VP. Of course, I'm just using standard pseudo-range on carrier phase. So it could be done by another receiver.

CLARK: I was going to ask which firmware did you use?

GIFFARD: It's 8.9 or 10, I'm not sure. It is important to get beyond 8.9.

BOYD MOORE (ITT Industries): Because solar flux affects ephemeris drastically, right? For lower orbits, I don't know about that height. I wonder if there is a correlation between solar flux affecting your TEV and ephemeris. Could you comment on that?

GIFFARD: I don't think I can comment on that. I'm sort of focused on producing a real-time answer, so I don't have time with this equipment. I can't calculate autonomous orbits or anything like that. So if there were such an effect, that would certainly spoil the result.